SIMULATION OF THE ELECTROMECHANICAL REPSONSE OF SELF-SENSING CARBON NANOTUBE POLYMER NANOCOMPOSITES

Miguel A.S. Matos[1], Vito L. Tagarielli[2] and Silvestre T. Pinho[3]

Department of Aeronautics, Imperial College London, South Kensington Campus,
London SW7 2AZ, United Kingdom
[1] miguel.matos@imperial.ac.uk
[2] v.tagarielli@imperial.ac.uk
[3] silvestre.pinho@imperial.ac.uk

Keywords: Nanocomposites, Strain sensing, Finite element model

ABSTRACT

A novel finite element approach to simulate the electromechanical properties and strain sensing capabilities of carbon nanotube polymer composites is presented. The models capture the nanoscale tunneling effect and its sensitivity to the imposed strain field. The approach is based on mechanical and electrical simulations of a representative volume element constructed based on measurable statistical descriptors of the microstructure. 2D and 3D approaches are described and resulting homogenized properties compared. Predictions are found in good agreement with previously published data.

1. INTRODUCTION

The use of carbon nanotubes (CNT) as a polymer composite filler has received outstanding interest due to their unmatched combination of mechanical, electrical and thermal properties [1]. Furthermore, their small dimensions, very high aspect ratios and low density enable augmentation of the composite properties at low concentrations [2], opening doors to the development of novel multifunctional materials for distinct applications [3]. Remarkably high stiffness in the range of 1 TPa has been reported for individual nanotubes [4]. Moreover, they can enable electrical conductivity in polymeric matrices with small concentrations, as low as 0.0025 wt% [5]. Due to their characteristics, these conductive composites display changes in conductivity when strained, operating as a self-sensing material that goes beyond some limitations of ordinary resistance strain gauges by being an embedded and multidirectional sensor [6] with superior sensitivities [7].

In this work, we present a multi-scale numerical approach that can capture the main mechanisms responsible for the conductivity of CNT-polymer composites and their sensitivity to deformation, and that can reproduce the geometric details of CNT dispersions. The mechanical and electrical properties of the material are calculated based on representative volume elements (RVE) constructed from statistical descriptors of the nanostructure. The developed framework considers both straight and curved CNTs in two- (2D) and three-dimensional (3D) domains. Geometry periodicity is enforced and different FE analyses, mechanical and electrical, are sequentially performed on the RVEs using Abaqus [8], both with periodic boundary conditions. The models can capture the nanoscale tunneling effect and its sensitivity to the imposed strain field, affecting the conductivity of the composite. Such effects are implemented using user-defined elements.

After determining the appropriate size of the RVE, homogenized mechanical and electrical properties are calculated and compared to published data. To conclude, the mechanical and electrical models are coupled to model the sensitivity of electrical conductivity to imposed strain, reproducing the piezoresistive behavior of these materials.

2. NUMERICAL MODELLING

All the FE models are based on the simulation of the electromechanical response of an RVE where nanotubes are dispersed according to statistical quantities retrieved from electron microscope observations. Two- and three-dimensional domains are considered.

After prescribing the target volume fraction V_f and defining the distributions for the nanotube dimensions – such as length L_CNT and external diameter D_CNT – and orientation, the wavy nanotubes are generated from a sequence of straight segments seeded at a random location within the RVE of side L_RVE. The first segment is aligned with the azimuthal α_0 and latitudinal ϕ_0 angles and each subsequent segment i has an angle $\theta_i \leq \theta_\mathrm{max}$ with the previous one. An illustration of this process is described in Figure 1. The waviness λ of the nanotubes is therefore controlled by prescribing the maximum angle θ_max and quantified as the ratio between its real and effective length L_eff defined as the distance between the start and end points:

$$\lambda = \frac{L_\mathrm{CNT}}{L_\mathrm{eff}} \tag{1}$$

The segments are then replaced by B-splines that share the same intermediate points and a check for intersections is performed. While intersections are allowed in 2D distributions, the nanotubes are indented in 3D, so that the tubular structures that describe them do not penetrate each other and the distance that separates them is never inferior to a specified d_min. Geometrical periodicity is subsequently enforced by repositioning the parts that override the domain boundaries.

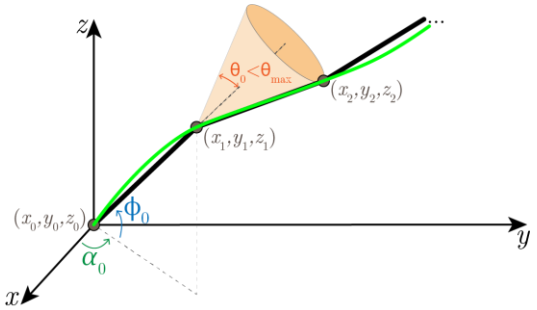

Figure 1: Illustration of the generation of a CNT distribution.

3. MECHANICAL PROPERTIES

From the generated nanostructure, the mechanical properties are calculated applying computational homogenization using the FE method. The macroscopic material can be idealized as a periodic repetition of the RVE along all Cartesian directions. Therefore, after discretizing the geometries of the polymeric matrix and nanotubes, periodic boundary conditions are prescribed. The RVE is then deformed by prescribing the macroscopic (homogenized) strain.

3.1. FE model and Homogenization

The nanotubes are modeled as equivalent continuum fibers [9] and therefore described as hollow cylinders discretized with B21 (2D) or B31 (3D) beam elements. The section of these elements has the same diameter of the nanotubes and the thickness of each nanotube wall is set to 0.34 nm [10], the interlayer thickness of graphene. Their behavior is considered linear isotropic with material properties (effective Young's modulus and Poisson's ratio) retrieved from either experiments or atomistic scale simulations.

The polymeric matrix is discretized into a regular mesh of 4 node plane strain (CPE4) or 8 node brick (C3D8) elements in the 2 or 3D cases, respectively. For the first, the plane strain elements have a thickness equal to the CNT diameter.

Aiming at small strains, the nanotubes are perfectly bonded to the matrix and modeled as embedded elements. For the 2D model, a duplicate node is introduced at all intersection points between distinct nanotubes so that forces and moments are not directly transferred from one to the other.

Periodic boundary conditions [11] are prescribed and six (or three in 2D) load cases – three (two) corresponding to uniaxial strain along each Cartesian direction and three (one) corresponding to pure shear loading – are created to retrieve the homogenized stiffness matrix. The full stiffness matrix can then be related with the homogenized Young's modulus $\bar{E}_\mathrm{comp}$ and Poisson's ratio $\bar{\nu}_\mathrm{comp}$.

3.2. Material Properties

In order to validate the current approach, we will consider the material properties and CNT distribution described by Yuan and Lu [12], with a 1% volume fraction of single wall carbon nanotubes (SWNT) randomly distributed in a Polypropylene (PP) matrix. All nanotubes are considered to have an outer diameter of $D_{\mathrm{CNT}} = 10$ nm and a length of $L_{\mathrm{CNT}} = 462$ nm, the average value referred by the same authors. As for the elastic properties, the SWNTs and PP matrix have modulus of 1 TPa and 1.756 Gpa with Poisson's ratio of 0.2 and 0.4, respectively.

4. ELECTRICAL PROPERTIES

The same RVE nanostructure and realization can be used to evaluate the electrical properties of the macroscopic composite material. Since CNTs are good conductors, their dispersion within an insulating matrix will result in a conductive material as long as they form a conductive (percolating) network. Due to the large range of conductivity of its parts, there is a concentration threshold above which the composite is said to be conductive – the critical volume fraction $V_{\mathrm{f_c}}$. The macroscopic conductivity will therefore depend on the intrinsic conductivity of the nanotubes, the pathway they form and the resistance between them. While the conductivity of the polymer matrix is often neglected due to the low typical values and increased modelling complexity, the presented methodology allows the inclusion of all.

4.1. Tunneling conductivity

Several authors have found experimental evidence [13] that the conductivity between adjacent CNTs is due to fluctuation-induced tunnelling electron transport. This conductivity depends on the probability of their electrons to penetrate and overcome the potential barrier created by the polymeric matrix and is here calculated using Simmons's generalized formula [14]. This formulation is also used to compute the electrical contact resistance between two nanotubes with a separation s coinciding with the van der Waals distance of 0.34 nm as it agrees with the value range measured for intersecting SWNTs [15].

4.2. FE model and Homogenization

Once again, the matrix is represented by a regular mesh where the nanotubes, described by continuum cylinders, are embedded. This is done by constraining the embedded CNT nodes to the matrix host elements by relating the position of the former and the interpolation functions of the latter.

The electrical analysis is performed using Abaqus heat-transfer analysis since the constitutive equations for electrical and thermal conductivity are analogous [16], replacing all thermal properties with the adequate electrical equivalents. In 2D, the matrix and nanotubes are discretized into DC2D4 planar 4-node and DC1D2 2-node link heat transfer elements, respectively. In 3D, the matrix elements are replaced by DC3D8 brick 8-node elements.

The tunneling resistance is modeled with a 2-node and 1 degree-of-freedom (DOF) per node user element (UEL subroutine [8]). It is applied at every contact location and at the closest distance between distinct nanotubes, when it is inferior to $d_{\mathrm{search}} = D_{\mathrm{CNT}} + d_{\mathrm{cut\text{-}off}}$, with a cut-off distance of $d_{\mathrm{cut\text{-}off}} = 4$ nm.

Periodic boundary conditions are applied via a constant electric field (or voltage potential) along each of the Cartesian directions in individual load steps. This allows for the reconstruction of all entries of the electrical conductivity matrix $\bar{\kappa}_{ij}$.

4.3. Material Properties

The presented methodology will be used to predict the electrical conductivity of a polymer nanocomposite with multi-wall nanotube (MWNT) fillers, randomly oriented in 2D and 3D domains. For validation purposes, the material properties discussed by Hu et al. [17] are considered: a random dispersion of CNTs with $D_{\mathrm{CNT}} = 50$ nm and $L_{\mathrm{CNT}} = 5$ μm in an epoxy matrix.

Regarding electrical properties, the examples consider a nanotube conductivity of 10^4 S/m and a small value of 10^{-6} S/m for the matrix. A relative permittivity of 3.98 is used for the latter. Since

Shiraishi and Ata [18] reported work functions of 4.95 and 5.05 eV for SWNT and MWNT, respectively, the last value is here considered.

5. STRAIN-SENSING

As discussed by Alamusi et al. [19], the piezoresistivity of carbon nanotube reinforced polymers is attributed to three mechanisms: (1) the destruction of conductive paths, (2) the change of inter-filler distances and (3) the inherent piezoresistivity of the CNTs. The contribution of the latter is often neglected, estimated to represent only 5% [20] of the overall change in resistance. Therefore, the current approach will focus only on the first two and dominant mechanisms.

To model the piezo-resistive response of the composite, the mechanical and electrical models are coupled sequentially. In the first, the sensitivity $\partial s/\partial \bar{\varepsilon}_i$ of the tunneling distances s with each of the six homogenized strain components $\bar{\varepsilon}_i$ is retrieved for every tunneling location. These sensitivities are then included in the electrical analysis where 6 global DOFs corresponding to the referred strain components control the extension of the tunneling distances.

Given the high number of nanotube intersections present in 2D models, the resulting piezoresistivity severely depends on the characteristics of each realization, since intersections can not be disconnected with deformation. For this reason, the presented results for strain-sensing refer only to 3D realizations.

6. RESULTS AND DISCUSSION

6.1 Elastic Properties

To compare and validate the 2D and 3D approaches, the homogenized elastic modulus of a SWNT-PP composite is now considered for different CNT waviness values.

Convergence studies for RVE size and mesh refinement were carried out, leading to RVE with sizes $L_{\mathrm{RVE}}^{\mathrm{2D}} = 5{\times}L_{\mathrm{CNT}}$ and $L_{\mathrm{RVE}}^{\mathrm{3D}} = 1.5{\times}L_{\mathrm{CNT}}$, both with approximately 0.8 million DOFs.

While keeping constant the total length of the nanotubes, the maximum angle between consecutive segments $\theta_{\max}$ was varied from 0° to 20° and the respective effective elastic modulus plotted against the waviness ratio in Figure 2. Since the filler distribution is approximately isotropic, the displayed values are averaged values of the Young's modulus retrieved along all Cartesian directions.

Analysing the results for a distribution of straight CNTs ($\lambda = 1$), averages of $\bar{E}_{\mathrm{comp}}^{\mathrm{2D}} = 1.889$ GPa and $\bar{E}_{\mathrm{comp}}^{\mathrm{3D}} = 1.941$ are obtained, whereas Yuan and Lu [12] have reported a value of 1.937 GPa with 3D FE simulations performed on an RVE with the nanotubes depicted by a tubular model, very close to the current predictions. Figure 2 shows that the effective modulus of the composite decreases with the CNT waviness for both approaches, with the 2D results being approximately 2.5% lower than the 3D. The descent slope agree with the predictions obtained by the same authors [12]. This trend can be explained by the fact that, while a straight CNT reinforcement acts only along its axis, it will also contribute to the transverse direction for a wavy geometry.

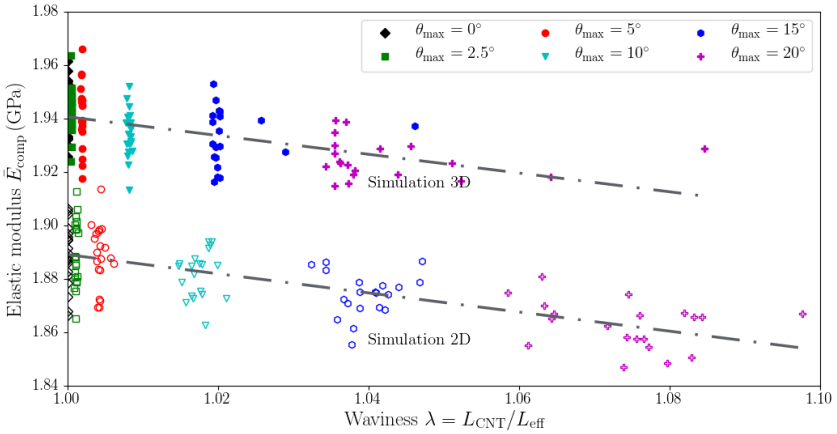

Figure 2: Influence of the CNT waviness on the homogenized elastic modulus of the composite for both 2D and 3D approaches.

6.2 Electrical Conductivity

The effects of the filler fraction on the electrical conductivity of the composite are now investigated. For the current analysis, RVEs of size $L_{\mathrm{RVE}}^{\mathrm{2D}} = 10{\times}L_{\mathrm{CNT}}$ and $L_{\mathrm{RVE}}^{\mathrm{3D}} = 1.5{\times}L_{\mathrm{CNT}}$ were chosen, considered to be representative of an isotropic nanotube distribution while leading to models with low computational costs. The resulting homogenized isotropic conductivities $\bar{\kappa}_{\mathrm{comp}}$ are plotted in Figure 3.

Comparing Figure 3a and Figure 3b, it is clear that a 2D approach should be applied exclusively to 2D distributions. While the 2D simulations predicts a percolation threshold (or critical volume fraction) of $V_{\mathrm{fr_c}}^{\mathrm{2D}} \simeq 4.0\%$, the 3D simulations place this threshold at around $V_{\mathrm{fr_c}}^{\mathrm{3D}} \simeq 0.6\%$. These values are close to the predictions obtained using the excluded volume theory [21] of 0.617% and 4.37% considering quasi-two-dimensional rod networks [22] and capped cylinders [21], respectively. The fact that the values here obtained are slightly lower can be easily justified by the inclusion of the tunnelling conductivity. Furthermore, it can be noted that both cases exhibit a region around the percolation threshold where the standard deviation of the obtained conductivity is very high. Since, at this critical volume fraction, the CNTs start to form an infinite cluster, the characteristic length of the problem tends to infinity at this point according to the percolation theory [23] and the anisotropy of the RVE is also maximum. Consequentially, it is expected that the critical RVE size tends to infinity around this threshold and that the change from low to high conductivity becomes more abrupt if the RVE size is increased.

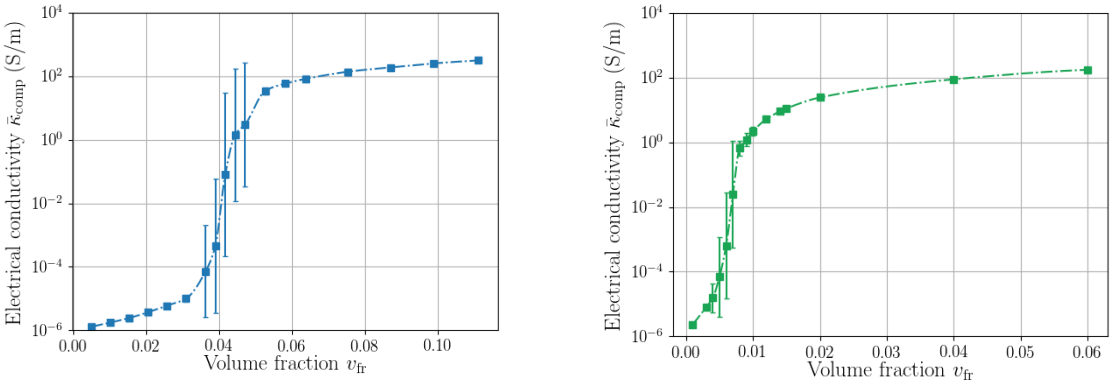

Figure 3: Homogenized electrical conductivity and respective standard deviation of the nanocomposite as function of the filler volume fraction for a: a) 2D and b) 3D CNT distribution.

6.3 Strain-sensing

The current section illustrates the integration of both physics into a single sequential analysis to reproduce the strain-sensing behaviour of a MWNT-epoxy composite with a volume fraction of 1%. The employed properties are the same used in the previous section with a nanotube total wall thickness of 5 nm. The electrical properties of such composite are the same as described in Figure 3b.

A uniform electric field is applied along each of the Cartesian directions and the RVE is loaded in the same direction in uniaxial stress. The measured change in resistance ΔR normalized by the initial resistance R_0 is plotted in Figure 4, for an RVE of size $L_{\mathrm{RVE}}^{\mathrm{3D}} = 3{\times}L_{\mathrm{CNT}}$.

It is clear the capability of the current models to simulate the increase in resistivity with tensile deformation and the obtained gauge factor $\mathrm{GF} = \frac{\Delta R}{R_0 \varepsilon}$ of approximately 30 at 6% strain is in the same order of magnitude of computational and experimental values reported in the literature for an equivalent weight fraction [7, 24, 25].

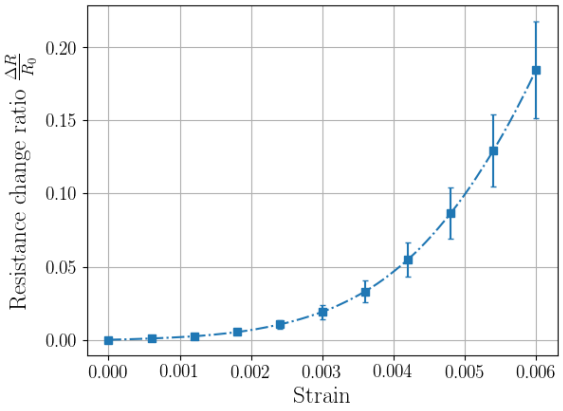

Figure 4: Simulated piezoresistivity of a MWNT-epoxy composite with 1% volume fraction for uniaxial stress with the electric field applied along the load direction

7. CONCLUSIONS

A finite element based framework has been developed to simultaneously retrieve the mechanical, electrical and piezoresistive properties of CNT-polymer composites. Using the FE method, periodic 2D and 3D RVEs have been simulated by concurrent electrical and mechanical FE analysis, later coupled to calculate the effects of strain on the electrical conductivity. The models reproduce the lower scale effect of tunneling conductivity.

A good agreement has been found between the calculated homogenized elastic properties and published results. As for the electrical quantities, the models were successful in predicting the conductivity for a variety of volume fractions and demonstrated the clear differences between 2D and 3D CNT distributions. The calculated percolation thresholds agree with the predictions obtained with the excluded volume theory. Furthermore, the piezoresistivity of such composites was numerically identified with gauge factors with the same order of magnitude of published data.

The presented workflow can integrate the different physics and respective coupling effects of these problems into a FE framework, raising the advantages of the latter. This enables the simulation of diverse nanostructures that can be characterized by statistical descriptors and the study of the effects of several distribution aspects on the macroscopic electromechanical properties of the composite

ACKNOWLEDGMENETS

This project has received funding from the European Union's Horizon 2020 research and innovation program under the Marie Skłodowska-Curie Grant Agreement no. 642890 (http://thelink-project.eu).

REFERENCES

[1] J. N. Coleman, *et al.* 2006. "Small but strong: A review of the mechanical properties of carbon nanotube-polymer composites," *Carbon*, **44** (9), 1624-1652.

[2] X. L. Xie, *et al.* 2005. "Dispersion and alignment of carbon nanotubes in polymer matrix: A review," *Materials Science & Engineering R-Reports*, **49** (4), 89-112.

[3] R. H. Baughman, *et al.* 2002. "Carbon nanotubes - the route toward applications," *Science*, **297** (5582), 787-792.

[4] M. M. J. Treacy, *et al.* 1996. "Exceptionally high Young's modulus observed for individual carbon nanotubes," *Nature*, **381** (6584), 678-680.

[5] J. K. W. Sandler, *et al.* 2003. "Ultra-low electrical percolation threshold in carbon-nanotube-epoxy composites," *Polymer*, **44** (19), 5893-5899.

[6] W. Obitayo and T. Liu. 2012. "A Review: Carbon Nanotube-Based Piezoresistive Strain Sensors," *Journal of Sensors*, 15.

[7] G. T. Pham, *et al.* 2008. "Processing and modeling of conductive thermoplastic/carbon nanotube films for strain sensing," *Composites Part B-Engineering,* **39** (1), 209-216.
[8] D. S. Simulia, *Abaqus 2017 Documentation*, 2017.
[9] E. T. Thostenson and T. W. Chou. 2003. "On the elastic properties of carbon nanotube-based composites: modelling and characterization," *Journal of Physics D-Applied Physics,* **36** (5), 573-582.
[10] G. M. Odegard, *et al.* 2002. "Equivalent-continuum modeling of nano-structured materials," *Composites Science and Technology,* **62** (14), 1869-1880.
[11] L. Gigliotti and S. T. Pinho. 2015. "Exploiting symmetries in solid-to-shell homogenization, with application to periodic pin-reinforced sandwich structures," *Composite Structures,* **132**, 995-1005.
[12] Z. Yuan and Z. Lu. 2014. "Numerical analysis of elastic–plastic properties of polymer composite reinforced by wavy and random CNTs," *Computational Materials Science,* **95**, 610-619.
[13] B. E. Kilbride, *et al.* 2002. "Experimental observation of scaling laws for alternating current and direct current conductivity in polymer-carbon nanotube composite thin films," *Journal of Applied Physics,* **92** (7), 4024-4030.
[14] J. G. Simmons. 1964. "Generalized Thermal J‐V Characteristic for the Electric Tunnel Effect," *Journal of Applied Physics,* **35** (9), 2655-2658.
[15] M. S. Fuhrer, *et al.* 2000. "Crossed Nanotube Junctions," *Science,* **288** (5465), 494-497.
[16] J. N. Reddy, *An Introduction To The Finite Element Method*: McGraw-Hill, 2006.
[17] N. Hu, *et al.* 2008. "Tunneling effect in a polymer/carbon nanotube nanocomposite strain sensor," *Acta Materialia,* **56** (13), 2929-2936.
[18] M. Shiraishi and M. Ata. 2001. "Work function of carbon nanotubes," *Carbon,* **39** (12), 1913-1917.
[19] Alamusi, *et al.* 2011. "Piezoresistive Strain Sensors Made from Carbon Nanotubes Based Polymer Nanocomposites," *Sensors,* **11** (11), 10691-10723.
[20] A. I. Oliva-Aviles, *et al.* 2013. "On the contribution of carbon nanotube deformation to piezoresistivity of carbon nanotube/polymer composites," *Composites Part B-Engineering,* **47**, 200-206.
[21] I. Balberg, *et al.* 1984. "Excluded volume and its relation to the onset of percolation," *Physical Review B,* **30** (7), 3933-3943.
[22] R. M. Mutiso and K. I. Winey. 2013. "Electrical percolation in quasi-two-dimensional metal nanowire networks for transparent conductors," *Physical Review E,* **88** (3)
[23] D. Stauffer and A. Aharony, *Introduction To Percolation Theory*: Taylor & Francis, 2003.
[24] N. Hu, *et al.* 2010. "Investigation on sensitivity of a polymer/carbon nanotube composite strain sensor," *Carbon,* **48** (3), 680-687.
[25] S. Gong and Z. H. Zhu. 2014. "On the mechanism of piezoresistivity of carbon nanotube polymer composites," *Polymer,* **55** (16), 4136-4149.